Organic LETTERS

Letter

pubs.acs.org/OrgLett

Chelation-Assisted Photoelimination of B,N-Heterocycles

Soo-Byung Ko,[†] Jia-Sheng Lu,[†] and Suning Wang*

Department of Chemistry, Queen's University, Kingston, Ontario K7L 3N6, Canada

Supporting Information

ABSTRACT: Metal-chelation and internal H bonds have been found to greatly enhance the photoelimination quantum efficiency of B,N-heterocycles by 2 orders of magnitude. Green phosphorescent Pt(II)-functionalized 1,2-azaborines have been achieved via photoelimination. A mechanistic pathway for the PE reaction has been established.

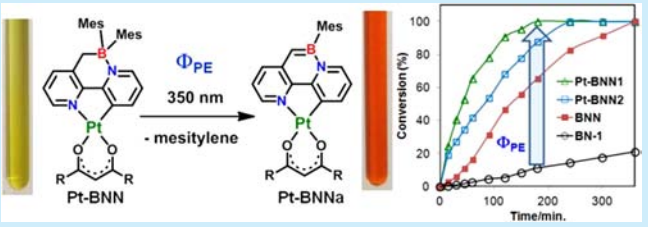

Incorporating a boron atom in conjugated organic molecules is known to be highly effective in generating new materials with versatile applications including sensory and optoelectronic/photoresponsive materials[1−4] and devices.[5] In particular, replacing a C−C unit with an isoelectronic B−N unit in aromatic compounds leads to the formation of azaborine and its derivatives,[6] which possess interesting electronic, photophysical, and chemical properties that are distinct from those of the isoelectronic C−C analogues, leading to many potential applications.[6,7] Thus, there is great interest in the chemistry of azaborine and derivatives and the development of efficient synthetic methods for new B,N-substituted aromatic compounds. We reported recently that B,N-heterocycles such as BN-1 shown in Scheme 1 can undergo an unusual photo-

Scheme 1. Proposed PE Pathway of B,N-Heterocycles

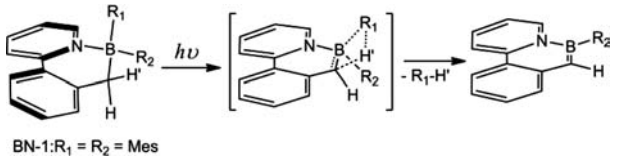

BN-1:$R_1 = R_2$ = Mes

elimination (PE) reaction in solution or in doped polymer films, generating B,N-substituted azaboraphenanthrenes in high yields.[8] This unusual reaction provides a convenient means for the synthesis of new B,N-substituted aromatic compounds that would be difficult to synthesize via alternative stepwise chemical reactions.[6,7] Nonetheless, in order to achieve moderate PE quantum efficiency (Φ_{PE}), the reactions in the previously reported systems require excitation at 300 nm, which can be very destructive to certain polymer hosts, thus limiting the use of the PE method in an in situ generation of patterned films for organic optoelectronics. Furthermore, the impact of metal ions on the PE process of B,N-heterocycles is not known. If metal-containing B,N-heterocycles can undergo a similar PE reaction as the parent ligand does, it would allow us to access previously unknown phosphorescent azaborine molecules, which have potential applications in OLEDs as phosphorescent dopants[5] and in phosphorescence-based sensing applications.[9] With the aim of examining the generality of the PE reaction in metal-containing systems to develop phosphorescent azaborines, to shift the PE excitation energy to a longer wavelength, and to enhance Φ_{PE}, a new BNN system shown in Scheme 2 was

Scheme 2. New BNN System

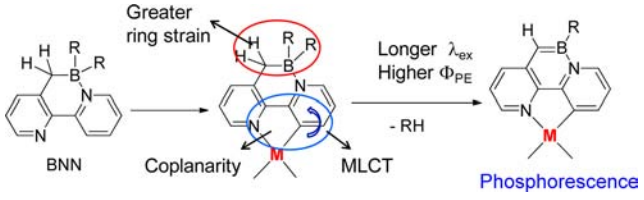

designed, and its Pt(II) chelate complexes were obtained. An investigation on the new system led to several surprising findings including the more than 100 times greater Φ_{PE} of the new system at 350 nm excitation, compared to BN-1, and the establishment of the reaction pathway shown in Scheme 1. The details are reported herein.

The precursor B,N-heterocycle BNN was designed on the basis of the consideration that it allows the attachment of a metal-chelate unit on the backbone via cyclometalation, which can introduce low energy states such as MLCT, thus potentially decreasing the excitation energy of the PE. BNN was prepared by the reaction of 3-methyl-2,2′-bipyridine with *n*-BuLi at −78 °C in the presence of TMEDA, followed by the addition of $BMes_2F$ (Scheme 3). The metal unit selected for attaching to BNN is Pt(acac) and the *tert*-butyl-substituted analogue Pt(tmhd) (tmhd = 2,2,6,6-tetramethyl-3,5-heptanedionate), based on the fact that N,C-chelate Pt(acac) or Pt(tmhd) compounds can produce bright phosphorescence.[5a,b] Pt−BNN1 and Pt−BNN2 were obtained in good yields (85−88%) by a modified one-pot cyclometalation procedure reported previously[10] at ambient temperature. BNN and its Pt(II) compounds were fully characterized by ^{1}H, ^{11}B, and ^{13}C

Received: December 8, 2013
Published: December 27, 2013

   dx.doi.org/10.1021/ol403550b | *Org. Lett.* 2014, 16, 616−619

Scheme 3. Synthetic Procedures of BNN, Pt−BNN1, Pt−BNN2, and Their B,N-Benzoquinolines

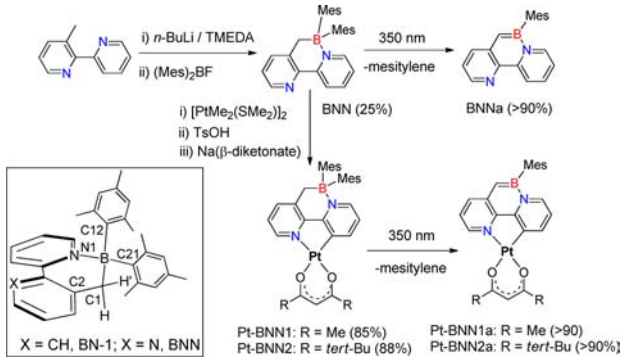

NMR spectra and HRMS/elemental analysis. The crystal structures of BNN and Pt−BNN2 were determined by single-crystal X-ray diffraction analysis.[11]

As shown by the crystal structures of BNN and Pt−BNN2 in Figure 1, the carbon atom (C(21), equatorial) of one of the

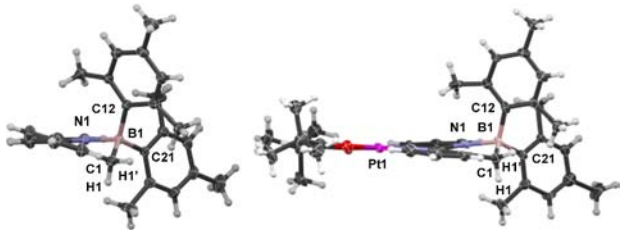

Figure 1. Crystal structure of **BNN** (left) and **Pt−BNN2** (right).

mesityl rings is approximately in the same plane with the bpy unit and the B,N-heterocycle, while the other carbon atom (C(12), axial) from the second mesityl is approximately perpendicular to it. The shortest separation distance between the H atoms of the CH_2 group and the carbon atoms of the mesityls is between C(12) and H(1′) (the *syn*-H atom). The bond lengths and angles around the Pt(II) center in Pt−BNN2 are typical and similar to those of the previously reported Pt(ppy)(acac) and derivatives.[5] The key difference between the structures of BN-1, BNN, and Pt-BNN2 is the torsion angle (N1CCC2, see Scheme 3) between the two chelate aryl rings (the bpy unit in BNN and Pt−BNN2, the ppy unit in BN-1), which decreases from BN-1 (26.7°) to BNN (22.9(2)°) due to an intramolecular N(2)···H bond (2.48 Å)[12] in BNN and to Pt−BNN2 (10.3(9)°) due to chelation. As a consequence, there is an increased coplanarity of the chelate unit with the B(1) and C(1) atoms from BN-1, BNN to Pt−BNN2. Further, the C(12) and H(1′) distance decreases from BN-1 (2.81 Å), BNN (2.73 Å) to Pt−BNN2 (2.65 Å), accompanied by more than 10° decrease of the C(12)−B(1)−C(1)−H(1′) torsion angle. The optimized structures of BN-1, BNN, Pt−BNN1, and Pt−BNN2 by DFT show a similar trend (Table S16a, Supporting Information). On the basis of the structural data, if the PE process indeed follows the pathway shown in Scheme 1 by eliminating R_1 and H′(C(12) and H(1′) in BNN and Pt−BNN2), it is conceivable that the Φ_{PE} of the reaction would follow the order of BN-1 < BNN < Pt−BNN1 ≈ Pt−BNN2, since the increased ring strain of the B,N-heterocycle and the reduced separation distance between C(12) and H(1′) can lead to a reduction in activation barrier toward photoelimination and the enhancement of Φ_{PE}.

The photoreactivity of BNN, Pt−BNN1, and Pt−BNN2 was examined by UV−vis, fluorescence/phosphorescence, and NMR spectra. As shown in Figures 2 and 3, the absorption

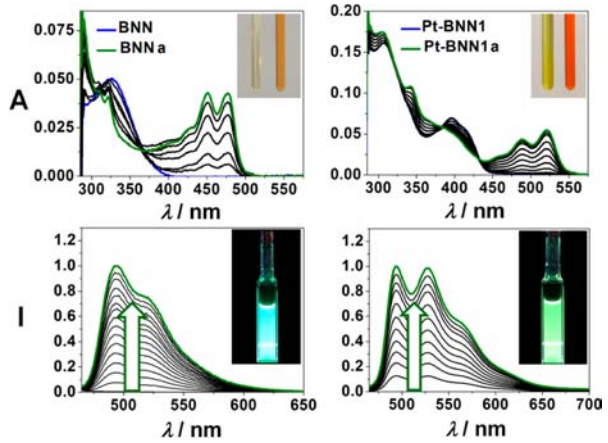

Figure 2. UV−vis (top) and emission (bottom) spectra showing the conversion of BNN and Pt−BNN1 in toluene (1.0×10^{-5} M) to their corresponding benzoquinoline compounds upon irradiation at 350 nm. Inset photographs show the color change (top) of the samples before and after irradiation and the emission color (bottom) of BNNa and Pt−BNN1a in toluene.

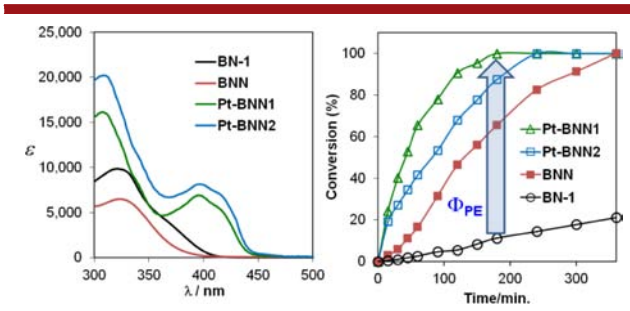

Figure 3. Left: absorption spectra of B,N-heterocycles in toluene. Right: a diagram showing the conversion percentage of the B,N-heterocycles to their corresponding B,N-benzoquinolines at 350 nm excitation (1.0×10^{-5} M in toluene).

spectra of Pt−BNN1 and Pt−BNN2 have a distinct low energy band at 380−450 nm that can be ascribed to MLCT and CT (mesityl to bpy) transitions, based on TD-DFT computational data (see the Supporting Information). BNN is nonemissive while both Pt(II) compounds display very weak green phosphorescence at ∼495 nm and $\Phi_{Phos.} \leq 0.01$. Upon irradiation at 350 nm under N_2 atmosphere in toluene or benzene (1.0×10^{-5} M), the color of the BNN solution changes gradually from colorless to light brown with the appearance of a new low energy absorption band at 400−510 nm (ε = 4300 M^{-1} cm^{-1}) with well-resolved vibrational features. In the fluorescence spectrum, a blue-green fluorescent peak appears that grows in intensity with time, as BNN is being irradiated at 350 nm (λ_{max} = 493 nm, $\Phi_{Fluor.}$ = 0.60 at 298 K; 478 nm at 77 K). The new species was designated as BNNa, an analogue of BN-1 and an isoelectronic species of 7,8-benzoquinoline. Compared to that of 7,8-benzoquinoline, the low energy absorption band and the fluorescent peak of BNNa are more than 100 nm red-shifted (see the Supporting Information), a trend commonly observed in B,N-substituted

dx.doi.org/10.1021/ol403550b | Org. Lett. 2014, 16, 616−619

aromatic compounds.[6,7] Under 350 nm excitation, both yellow solutions of Pt−BNN1 and Pt−BNN2 become red-orange with the appearance of a new low energy band at 440−560 nm (ε = 4300−7600 M^{-1} cm^{-1}) that was assigned to the new species Pt−BNN1a and Pt−BNN2a, respectively (Figure 2 and Supporting Information). In the phosphorescent spectra, the weak green phosphorescent peak gains intensity with irradiation time with more than 10-fold increase of the emission quantum efficiency (λ_{phos} = 0.13−0.14, τ = 12.7(3) −14.3(4) μs). The structures of BNNa, Pt−BNN1a, and Pt−BNN2a were established by 1D and 2D (NOESY) NMR spectroscopic analysis, which showed that BNN, Pt−BNN1, and Pt−BNN2 convert to BNNa, Pt−BNN1a, and Pt−BNN2a, respectively, in nearly quantitative yields (see the Supporting Information). The new azaborine compounds were isolated and characterized by HRMS and NMR. The ^{11}B NMR chemical shifts of BNNa, Pt−BNN1a, and Pt−BNN2a are at 35.7, 37.5, and 37.6 ppm, respectively, similar to those previously reported for 1,2-azaborine compounds[6,7] BN-1 and derivatives.[8] Efforts to obtain single crystals of BNNa, Pt−BNN1a, and Pt−BNN2a for X-ray diffraction analysis were unsuccessful. The UV−vis absorption and fluorescence spectra of BNN, Pt−BNN1, and Pt−BNN2 in poly(methylmethacrylate) (PMMA) films display a change similar to those recorded in toluene upon irradiation, supporting that the PE reaction of these compounds also occur in polymer hosts as observed for BN-1 and its derivatives but at a much lower excitation energy (350 nm) (see the Supporting Information).

Significantly, despite the presence of the low energy absorption band at λ_{max} = ∼400 nm for Pt−BNN1 and Pt−BNN2, excitation at 400 nm only led to very slow and inefficient PE (Φ_{PE} <0.001), indicative of a minimum excitation energy threshold required for the PE process. Compared to BN-1 and its derivatives that require 300 nm excitation to achieve moderate Φ_{PE} (0.044), the PE of BNN, Pt−BNN1, and Pt−BNN2 can proceed at 350 nm excitation with an impressive Φ_{PE} (0.045 for BNN to BNNa, 0.093 for Pt-BNN1 to Pt-BNN1a, and 0.080 for Pt−BNN2 to Pt−BNN2a). Remarkably, the Φ_{PE} of BNN is more than 100 times greater than that of BN-1 (<0.0001) at 350 nm excitation, despite the greater absorbance of BN-1 at 350 nm (Figure 3). For the Pt(II) compounds, the Φ_{PE} is even higher, nearly double that of BNN. Clearly, the greatly enhanced Φ_{PE} at 350 nm for BNN, Pt−BNN1, and Pt−BNN2 compared to BN-1 cannot be explained by the absorption intensity difference.

TD-DFT calculation results confirmed that the low energy absorption bands of BNNa, Pt−BNN1a, and Pt−BNN2a in the 420−550 nm region are indeed from a $\pi \rightarrow \pi^*$ (HOMO → LUMO) transition localized on the benzoquinoline ring with a high oscillator strength. The fluorescence of BNNa is most likely from the same transition. For Pt−BNN1a and Pt−BNN2a, the phosphorescence is most likely from the T_2 state involving a $\pi \rightarrow \pi^*$ transition of the benzoquinoline ring since it is necessary to excite these molecules at 395 nm that is beyond the low energy absorption band (440−550 nm) in order to observe the phosphorescence.

For the precursor compounds, TD-DFT data indicate the transition at the 350 nm excitation (3.54 eV) involves HOMO-4 → LUMO (S_6, 96%) for BNN, HOMO-7 → LUMO (S_9, 95%) for Pt−BNN1, and Pt−BNN2 (Figure 4). The BN-1 compound has a similar transition as that of BNN and for comparison purpose is also included in Figure 4. The LUMO level for BN-1, BNN, Pt−BNN1, and Pt−BNN2 is similar, a π^* orbital localized on the ppy or the bpy unit. The HOMO-4 or HOMO-7 level of these compounds contains π orbitals of the chelate unit, the d orbital of the Pt atom (13% for Pt−BNN1 and Pt−BNN2), and most significantly the σ orbitals of the C−H bond (the CH_2 unit) and the B−$C_{Mes(axial)}$ bond (C(12)) (27% for BN-1, 28% for BNN, 34% for Pt−BNN1) in addition to the B−CH_2 σ bond. Vertical excitations at energies below ∼3.54 eV have either no or very little C−H or B−C σ bond contributions. Thus, the photoexcitation of these molecules at ∼350 nm appears to be the minimum energy required to weaken the C−H and the B−$C_{Mes(axial)}$ bond in the PE process, providing a plausible explanation for the observed minimum excitation energy threshold. Notably, the σ orbital contributions of the C−H and B−$C_{Mes(axial)}$ bond in HOMO-7 of Pt−BNN1 and Pt−BNN2 are much greater than those in HOMO-4 of BNN, which could make the photoexcitation of the C−H and B−C bond more effective. Because there is little difference on the electronic structure of BN-1 and BNN, the great Φ_{PE} enhancement of BNN relative to BN-1 at 350 nm excitation can only be explained by the increased coplanarity of the bpy unit and the B,N-heterocycle caused by an internal N···H bond in BNN. The thermal elimination pathway was established by DFT computations for BN-1 and BNN and is shown in Figure 5. The optimized structure of the transition state involves an H atom that is midway between C(1) and B(1) atom and a detached Mes group that is ∼2.0 Å away from the B atom (see the Supporting Information for details). The computational

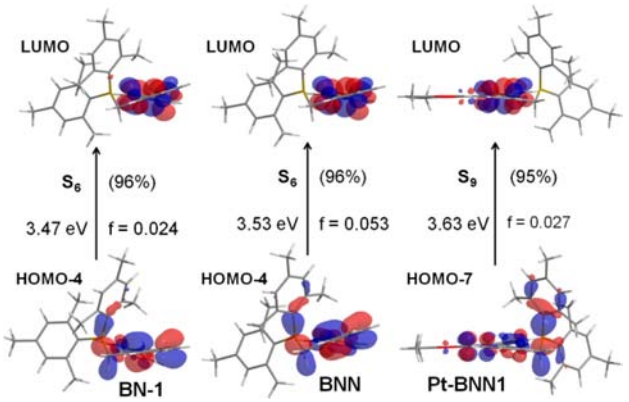

Figure 4. Orbitals involved in the vertical excitation of the B,N-heterocyclic compounds that are responsible for initiating the PE process.

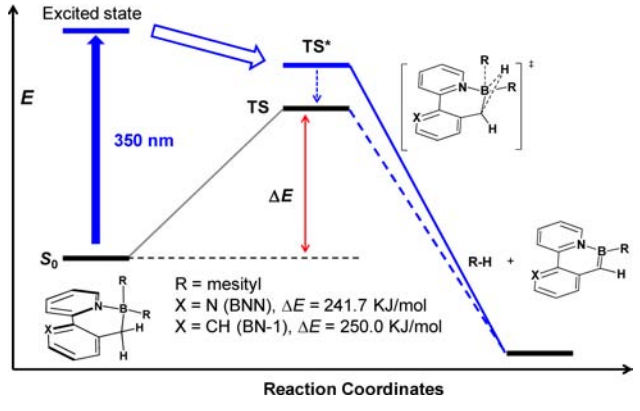

Figure 5. A diagram showing the relative energies of the reactant, the transition state and the products of the PE process.

dx.doi.org/10.1021/ol403550b | Org. Lett. 2014, 16, 616−619

data support that the PE reaction has to proceed through the excited state because of the large activation barrier, presumably involving a transition state that resembles the one in the thermal pathway. The activation barrier of BNN was found to be 8.3 kJ/mol lower than that of BN-1, supporting its greater PE reactivity.

In conclusion, new and highly phosphorescent B,N-benzoquinolines have been achieved via a PE process. Metal chelation and internal H bonds have been found to greatly enhance Φ_{PE} of B,N-heterocycles by reducing the activation barrier and lowering the excitation energy, although a minimum excitation energy threshold was found to be necessary in order to break the C−H and B−C bonds. The use of metal chelation/coordination to influence photochromic systems is known to be an effective approach by influencing the electronic state of the molecule.[13] This work is the first example demonstrating the impact of metal chelation on PE reactions in which geometric constraints play a major role.

■ ASSOCIATED CONTENT

Supporting Information

Synthetic details and characterization data for all compounds, crystal structural data, photophysical data, DFT/TD-DFT computational data, and NICS values. This material is available free of charge via the Internet at http://pubs.acs.org.

■ AUTHOR INFORMATION

Corresponding Author

*E-mail: wangs@chem.queensu.ca.

Author Contributions

†These authors contributed equally to the work reported here.

Notes

The authors declare no competing financial interest.

■ ACKNOWLEDGMENTS

We thank the Natural Sciences and Engineering Research Council of Canada for financial support. S.W. thanks the Canada Council for the Arts for the Killam Research Fellowship.

■ REFERENCES

(1) (a) Yamaguchi, S.; Shirasaka, T.; Akiyama, S.; Tamao, K. *J. Am. Chem. Soc.* **2002**, *124*, 8816−8817. (b) Zhou, G.; Baumgarten, M.; Müllen, K. *J. Am. Chem. Soc.* **2008**, *130*, 12477−12484. (c) Wade, C. R.; Broomsgrove, A. E. J.; Aldridge, S.; Gabbaï, F. P. *Chem. Rev.* **2010**, *110*, 3958−3984.

(2) (a) Chen, P.; Jäkle, F. *J. Am. Chem. Soc.* **2011**, *133*, 20142−20145. (b) Dou, C.; Saito, S.; Yamaguchi, S. *J. Am. Chem. Soc.* **2013**, *135*, 9346−9349. (c) Reus, C.; Weidlick, S.; Bolte, M.; Lerner, H.-W.; Wagner, M. *J. Am. Chem. Soc.* **2013**, *135*, 12892−12907.

(3) (a) Sun, Y.; Ross, N.; Zhao, S. B.; Huszarik, K.; Jia, W. L.; Wang, R. Y.; Macartney, D.; Wang, S. *J. Am. Chem. Soc.* **2007**, *129*, 7510−7511. (b) Hudson, Z. M.; Wang, S. *Acc. Chem. Res.* **2009**, *42*, 1584−1596. (c) Varlan, M.; Blight, B. A.; Wang, S. *Chem. Commun.* **2012**, *48*, 12059−12061.

(4) (a) Nagura, K.; Saito, S.; Fröhlich, R.; Glorius, F.; Yamaguchi, S. *Angew. Chem., Int. Ed.* **2012**, *51*, 7762−7766. (c) Araneda, J. F.; Neue, B.; Piers, W. E.; Parvez, M. *Angew. Chem., Int. Ed.* **2012**, *51*, 8546−8550. (d) Rao, Y. -L.; Amarne, H.; Chen, L. D.; Mosey, N. J.; Wang, S. *J. Am. Chem. Soc.* **2013**, *135*, 3407−3410. (e) Iida, A.; Saito, S.; Sasamori, T.; Yamaguchi, S. *Angew. Chem., Int. Ed.* **2013**, *52*, 3760−3764.

(5) (a) Hudson, Z. M.; Sun, C.; Helander, M. G.; Amarne, H.; Lu, Z. -H.; Wang, S. *Adv. Funct. Mater.* **2010**, *20*, 3426−3439. (b) Hudson, Z. M.; Sun, C.; Helander, M. G.; Chang, Y. -L.; Lu, Z. -H.; Wang, S. *J. Am. Chem. Soc.* **2012**, *134*, 13930−13933.

(6) (a) Campbell, P. G.; Abbey, E. R.; Neiner, D.; Grant, D. J.; Dixon, D. A.; Liu, S. -Y. *J. Am. Chem. Soc.* **2010**, *132*, 18048−18050. (b) Campbell, P. G.; Marwitz, A. J. V.; Liu, S. -Y. *Angew. Chem., Int. Ed.* **2012**, *51*, 6074−6092. (c) Neue, B.; Araneda, J. F.; Piers, W. E.; Parvez, M. *Angew. Chem., Int. Ed.* **2013**, *52*, 9966−9969.

(7) (a) Braunschweig, H.; Damme, A.; Jimenez-Halla, J. O. C.; Pfaffinger, B.; Radacki, K.; Wolf, J. *Angew. Chem., Int. Ed.* **2012**, *51*, 10034−10037. (b) Wang, X. -Y.; Lin, H. -R.; Lei, T.; Yang, D. -C.; Zhuang, F. -D.; Wang, J. -Y.; Yuan, S. -C.; Pei, J. *Angew. Chem., Int. Ed.* **2013**, *52*, 3117−3120.

(8) Lu, J. -S.; Ko, S. -B.; Walters, N. R.; Kang, Y.; Sauriol, F.; Wang, S. *Angew. Chem., Int. Ed.* **2013**, *52*, 4544−4548.

(9) (a) Sun, Y.; Wang, S. *Inorg. Chem.* **2010**, *49*, 4394−4404. (b) Ko, S. -B.; Lu, J. -S.; Kang, Y.; Wang, S. *Organometallics* **2013**, *32*, 599−608.

(10) Hudson, Z. M.; Blight, B. A.; Wang, S. *Org. Lett.* **2012**, *14*, 1700−1703.

(11) Crystal data of **BNN** and **Pt-BNN2** have been deposited with the Cambridge Crystallographic Data Centre (CCDC 959400 and 959401).

(12) For similar intramolecular N···H bonds, see: Yokoyama, D.; Sakaguchi, A.; Suzuki, M.; Adachi, C. *Appl. Phys. Lett.* **2009**, *95*, 243303.

(13) (a) Ko, C. C.; Yam, V. W. W. *J. Mater. Chem.* **2010**, *20*, 2063−2070 and references cited therein. (b) Wang, N.; Ko, S.-B.; Lu, J.-S.; Chen, L. D.; Wang, S. *Chem.—Eur. J.* **2013**, *19*, 5314−5323.